ChemComm

Phase Transformation Induced Mechanochromism in a Platinum Salt: A Tale of Two Polymorphs

Journal:	*ChemComm*
Manuscript ID	CC-COM-05-2020-003436.R2
Article Type:	Communication

COMMUNICATION

Phase Transformation Induced Mechanochromism in a Platinum Salt: A Tale of Two Polymorphs

Received 00th January 20xx,
Accepted 00th January 20xx

DOI: 10.1039/x0xx00000x

Amie E. Norton[a,b*], Mahmood Karimi Abdolmaleki[a,c], Jiamin Liang[a], Malvika Sharma[a], Robert Golsby[a], Ann Zoller[a], Jeanette A. Krause[a], and William B. Connick[a,d], Sayandev Chatterjee[e,f*]

Red crystals of $[Pt(tpy)Cl]NO_3 \bullet HNO_3$ show mechanochromic behaviour turning yellow when pressure is applied. The electronic character and spectroscopic signature of the red and yellow polymorphs change as a result of slipping of the molecular stacking planes in the solid state. The slippage alters the Pt•••Pt intermolecular distances from a linear stacked motif with <3.5 Å separations in the red polymorph to a stacked motif of alternating short intradimer and long interdimer interactions in the yellow polymorph.

''Smart'' mechano-responsive materials that change their properties upon exposure to a predefined mechanical stimulus in a highly selective and predictable manner are of considerable interest in applications ranging from mechanical force sensors,[1-4] mechano-catalysis,[5] self reinforcing materials,[6-7] and controlled release of small molecules.[8-9] Specifically, mechanochromic or mechanoluminescent materials that are based on predictable changes in the elecronic structures of the material at a molecular level, leading to customizable changes in their optical and luminescent properties upon application of a mechanical stimuli,[10-11] such as pressure, stretching,[12] or grinding,[13] are finding wide applications security systems,[14] or for detecting mechanical failure or breach in devices[15] or the loss of mechanical integrity.[16-17] Among small molecules, ionorganic coordination complexes consisting of a coordinatively unstaturated metal center such as Pt(II)[18] or Au(I)[19] metal centers have demonstrated such mechanochromic or mechanoluminescent behavior,[20] due to the ability of these molecules to form tunable M•••M interactions that can be modified in a predicted and desired manner by the appliation of the external mechanical stimuli. Grinding or rubbing these materials in solid states have resulted in changes in their color and emission spectroscopies due to the force induced structural rearrangement resulting in changes in the M•••M interactions.[21-24] These M•••M ineractions orchestrate the spectroscopies of these complexes; as a representative example in coordinatively unstaturated Pt(II) complexes with sterically permitting ligands that have strong σ-donating and π-accepting character (an example being 2,2';6',2''-terpyridine (henceforth referred to as tpy),[25-26] the shortening of non-covalent Pt•••Pt distances stabilizes MMLCT (Metal Metal Ligand Charge Transfer) [$d\sigma^*(Pt) \rightarrow \pi^*(tpy)$] states lead to intensification of colors and luminescence from these materials.[27-29]

Understanding and controlling mechanical stimuli of these materials to impact thier applications in chemical sensing requires detailed structural information on this behavior.[29-30] However, in instances, the availability of such detailed structural information is limited by (i) the inherent difficulty in isolating and extracting such information if only a subset of crystal lattice sites undergo structural rearrangement, as in the case of the formation of defects;[29-32] (ii) mechanical stimulation can interrupt long-range order in crystals in instances, thereby preventing characterization by single-crystal X-ray diffraction.[33-34] Zhang *et al*.[18] have attempted to address this problem in their investigations of several $Pt(Me_3SiC{\equiv}CbpyC{\equiv}CSiMe_3)(L)_2$ complexes with a 5,5'-*bis*(trimethylsilylethynyl)-2,2'-bipyridine chelate, where L is a para-substituted phenylacetylide ligand.[2-6] The X-ray diffractograms before and after grinding indicate that this mechanical stimulation causes conversion of the solid to an amorphous phase. From the red-shift in the emission spectrum, it was proposed that grinding results in a decrease in Pt•••Pt separation and stabilization of the MMLCT states. Despite these

[a.] *Department of Chemistry, University of Cincinnati, Cincinnati, OH, 45221*
[b.] *Present Address: USDA-ARS, 1515 College Avenue, Manhattan, KS, 66503*
[c.] *Present Address: Department of Biology and Chemistry, Texas A&M International University, Laredo, TX, 78041*
[d.] *Prof. Connick passed away on April 22, 2018. This paper is dedicated to his memory*
[e.] *Energy and Environment Directorate, Pacific Northwest National Laboratory, Richland, WA, 99352*
[f.] *Present Address: ESSENCE Diagnostics LLC, Livingston NJ 07039*
**Corresponding Authors: amie.norton@usda.gov; sayandev@essencediagnostics.com*

† Electronic Supplementary Information (ESI) available: Synthetic details, spectral data, structural mapping calculation details, and complete single-crystal (CCDC 1956908-1956909) X-ray diffraction details (CIF format). See DOI: 10.1039/x0xx00000x

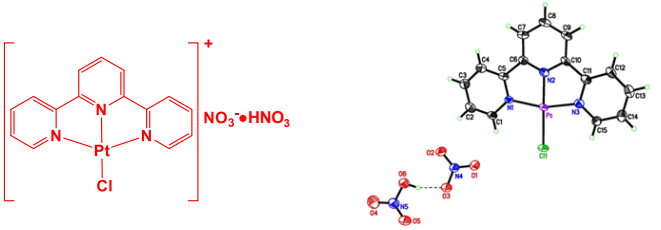

Fig. 1. (left) Molecular structure of the formula unit of the salt [Pt(tpy)Cl]NO_3•HNO_3 (**1**•NO_3•HNO_3). (right) ORTEP of **1**•NO_3•HNO_3.

efforts, the full details of structural rearrangement in this and other systems remain unknown.

Herein we report a mechanically-induced phase change in a single-crystal resulting in a change in color and luminescence properties. Specifically, [Pt(tpy)Cl]NO_3•HNO_3 (**1**•NO_3•HNO_3) (**Fig. 1**) turns from red to yellow when slight pressure is applied. The results reveal the structural basis for the mechanochromism in this system.

Red crystals of **1**•NO_3•HNO_3 were generated by evaporation of a solution of **1**•Cl•H_2O dissolved in a 1:1 mixture of 1M HNO_3 and acetone in ~1 day (synthesis and crystallizations described in Sections S1-S3, ESI). Slowing down the evaporation rate by an order of magnitude (7-10 days) yielded crystals of an yellow polymorph, whose chemical composition was confirmed by elemental analysis. The association of the HNO_3 solvate within the crystal structure of both the poymorphs were confirmed by ^{1}H NMR spectroscopy in DMSO (**Fig. S1, ESI**), IR measurements (**Table S1, ESI**) and mass spectrometry studies (**Fig. S2, ESI**). A simple physical contact of the red **1**•NO_3•HNO_3 polymorph with a needle resulted in an abrupt color change of the individual crystals from red to yellow as illustrated by the photographs shown in **Fig. 2(top)** of a representative crystal before and after contact with a needle. The chemical analysis of the crystals before and after being touched with a needle confirmed them to have the same chemical composition and crystal structure analysis, suggesting them to be two polymorphs, and indicating that a simple needle touch was able to induce a mechanical stimulation that resulted in the change in color from red to yellow. It is worth noting that the observed mechanochromic response was irreversible at shorter time periods, as the yellow form was observed to persist in the absence of any other external stimuli. However, when left for prolonged period (~45 days), the surface of the yellow polymorph demonstrated perturbations and gradually turned orange (shown in **Fig. S3, ESI**). This orange form was no longer mechanochromic as the orange color was observed to persist even on pressing the crystal with needle. Further, redissolution of the yellow crystals in 1:1 solution of acetone and 1M HNO_3 followed by their evaporation were observed to regenerate the red and yellow polymorphs depending upon the speed of evaporation.

In addition to confirming that the red and yellow crystals grown from solution have the same chemical composition, single-crystal X-ray diffraction studies (**Tables S2-S3; Figs. S4-S6, ESI**†) showed that yellow crystals grown from solution and those generated independently by subjecting the red crystals to a needle-touch, were in fact identical. Thus, the accumulated data is consistent with the existence of two polymorphs, namely the red and yellow forms of **1**•NO_3•HNO_3. Based on the rate of their appearance, the red form appears to be a kinetic product,

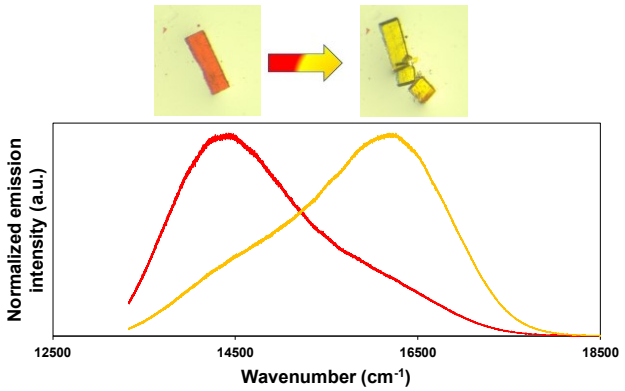

Fig. 2. (top) Photographs of a representative crystal of **1**•NO_3•HNO_3 (left) before and (right) after being touched with a needle. (bottom) Emission spectra (red trace,—) before touching and (yellow trace,—) after touching (λ_{ex} = 442 nm).

while the yellow form is assigned to be the thermodynamic product.

The observed color changes in the two polymorphs are directly related to the respective Pt•••Pt interactions in them. The red polymorph, crystallizing in triclinic, P-1 space group, shows stacked Pt(tpy)Cl$^+$ units arranged in a head-to-tail fashion producing an approximately linear continuous chain of uninterrupted Pt atoms along the *a*-axis with short Pt•••Pt distances alternating at 3.2845(4) and 3.3705(4) Å and a near-linear Pt•••Pt•••Pt angle of 161.22(1)° (**Fig. 3(a)**). The yellow polymorph, irrespective of whether it is grown freshly out of solution or is generated via a mechanically induced transformation, also coincidentally belongs to a P-1 space group with triclinic symmetry, but shows a greater calculated density, showing more efficient packing (**Fig. 3(b)**). Here, the Pt(tpy)Cl$^+$ units are arranged as head-to-tail dimers with short intradimer Pt•••Pt distances of 3.311(4) Å, but very long interdimer distances>7 Å. Thus, as opposed to the approximately linear chain arrangement of infinite Pt(tpy)Cl$^+$ cations in the red polymorph, the cations in the yellow polymorph can be described as head-to-tail dimers with short intradimer Pt•••Pt distances, but very long interdimer distances. The difference in the solid-state arrangement, dimers (yellow form) *vs.* linear chain (red form), is consistent with the observed colors.[39,40]

Emission spectroscopies of the two polymorphs reveal the difference in stabilities of the MMLCT (Metal Metal Ligand Charge Transfer) [$d\sigma^*(Pt)\rightarrow\pi^*(tpy)$] states in the two forms. As demonstrated previously in studies by Che et al. and Bailey et al. of similar [Pt(tpy)Cl]$^+$ complexes, these transitions are strongly dependent on the Pt•••Pt separation.[35, 37] The red polymorph showed an emission maximum near 700 nm (14400 cm^{-1}) (**Fig. 2, bottom red trace**). The red color and long wavelength emission of the "red" polymorph were consistent with low-lying spin-forbidden ^{3}MMLCT transitions (*vide-infra*).[35-36] These transitions in the "red" polymorph were consistent with stacked structure of an approximate linear chain of Pt atoms with relatively short non-covalent Pt•••Pt interactions (<3.5 Å), which was validated by the crystal structure of the polymorph (**Fig. 3**). Upon applying slight pressure, the crystal turned yellow and a new emission band was observed near 620 nm

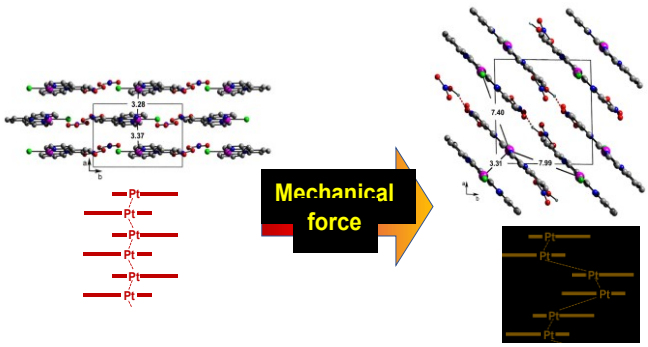

Fig. 3. Crystal structure stackings of the polymorphs of **1**•NO3•HNO3, with select Pt•••Pt distances in angstroms. H-atoms have been omitted for clarity: (left) red and (right) yellow polymorphs. The schematics with the Pt•••Pt interactions are represented below each respective ORTEP.

(16270 cm^{-1}) (**Fig. 2, bottom yellow trace**). This yellow transition is characteristic of ^{1}MMLCT transition (*vide infra*),[35, 37] that is expected to result from decrease in Pt•••Pt interactions in aggregating $[Pt(tpy)Cl]^{+}$ complexes in solid state. This is validated by the crystal structure of the yellow form showing sets of **Pt•••Pt** dimeric units (**Fig. 3**). Yellow crystals grown from solution also showed an emission maxima near 620 nm, and yellow powder formed by grinding red crystals exhibited an emission maximum near 610 nm. The bulk forms of the red and yellow forms also showed emissions consistent with the individual crystals. In fact, no discernible changes in the were observed in emission spectra of each polymorph irrespective of whether they were taken as a bulk powder form enclosed in quartz tubes, as microcrystals or in the form of thin films formed on quartz slides. (**Fig. S8, ESI**) As the red crystals were aged, either in or removed from the mother liquor, their emission spectra changed, gradually converging to that observed for the yellow crystals. For example, emission spectra of individual red crystals recorded just one day after precipitation from solution exhibited maxima or shoulders near both 620 and 690 nm. In other words, the spectra appeared to be a superposition of the spectra of freshly-prepared red crystals and yellow crystals. After 3 days in the mother liquor or air, the 700 nm feature was virtually absent from the spectra of the red crystals. The fact that the crystals retained their red color over this time period suggests that conversion of the red form to the yellow form occurs from the inside of the crystals and propagates toward the surface.

In order to understand how the red polymorph transforms to the yellow polymorph, we converted the unit cell of the yellow form into the red form (see calculation in **Section S4, ESI**†). Examination of the packing diagrams of the red and transformed yellow structures reveals the path of least molecular rearrangement required for interconversion. The extent of additional molecular rearrangement accompanying the phase change was assessed by determining the distances between the mapped structural elements. The $Pt(tpy)Cl^{+}$ columns in the red polymorph are uniformly further from the origin than those in the yellow polymorph, reflecting a slight contraction in the xz-plane upon red-to-yellow conversion. However, the area of the two-dimensional oblique lattice of the red polymorph is only 1.03% greater (%δA) than that of the yellow polymorph. Along the stacking axis, a complex falls completely out of register with its mapped counterpart every 767 Å (=h) or ~57 unit cells. This information also is captured by the unitless parameter ρ(z), which is the displacement of mapped Pt atoms (in Å) divided by the distance (in Å) of the Pt atom in the red polymorph from the origin. The value of ρ(z) is 0.017, which is consistent with a 1.72% expansion along z. For comparison, the maximum ρ value in the xy-plane, $\rho(xy)_{max}$, is ~0.005. Therefore, the percent contraction in volume (%δV) upon conversion from the red to yellow polymorph is only 1.62%. The overall good agreement between the two-dimensional lattices of columns of $Pt(tpy)Cl^{+}$ complexes and similar spacing of complexes along the stacking axis are likely important factors in the reason why the phase change is completed without significant loss of long-range order, which in turn allowed for single-crystal X-ray diffraction studies before and after mechanical stimulation.

Table 1. Parameters for mapping of **1**•NO_3•HNO_3

δa' (Å)	0.23
%δV (%)	1.62
$\rho(xy)_{max}$	0.05
ρ(z)	0.007

We have reported a new crystal-to-crystal phase change. The structure of both forms were determined using single-crystal X-ray diffraction. To the best of our knowledge, this is the first report of a structural analysis performed on a single crystal of a platinum(II) complex before and after a mechanically-induced change. The details outlined here provide insight into how mechanical stimuli induce changes in the spectroscopy of platinum(II) systems. This discovery of a new material with demonstrated mechanochromic behavior presents promise with potential applications in security systems to detect tampering, or for the detection of mechanical failure or the loss of mechanical integrity in devices.

Acknowledgements

This research was supported by (1) the STAR Fellowship Assistance Agreement FP-91765901 awarded by the U.S. Environmental Protection Agency (EPA) (A.E.N.), (2) the National Science Foundation (CHE-1152853) (W.B.C.), and (3) Laboratory Directed Research and Development Program (EED-SEED) at the Pacific Northwest National Laboratory operated by Battelle for the U.S. Department of Energy under Contract DE-AC05-76RL01830 (S.C.). Funding for the SMART6000 diffractometer was through NSF-MRI grant CHE-0215950. The views expressed in this publication are solely those of the publisher, and EPA does not endorse any products or commercial services mentioned in this publication.

Conflicts of interest

"There are no conflicts to declare".

References

1. Weder, C., *Journal of Materials Chemistry* **2011,** *21* (23), 8235-8236.

2. Grady, M. E.; Beiermann, B. A.; Moore, J. S.; Sottos, N. R., *Acs Appl Mater Inter* **2014,** *6* (8), 5350-5355.
3. Chen, G.; Cui, Y.; Chen, X., *Chemical Society Reviews* **2019,** *48* (6), 1434-1447.
4. Zhu, Q.; Van Vliet, K.; Holten-Andersen, N.; Miserez, A., A *Advanced Functional Materials* **2019,** *29* (14), 1808191.
5. Swager, T. M.; McDonald, B. R., *Synfacts* **2019,** *15* (06), 0611.
6. Jakobs, R. T. M.; Ma, S.; Sijbesma, R. P., *ACS Macro Lett* **2013,** *2* (7), 613-616.
7. Hou, Y.; Du, J.; Hou, J.; Shi, P.; Wang, K.; Zhang, S.; Han, T.; Li, Z., *Dyes and Pigments* **2019,** *160*, 830-838.
8. Larsen, M. B.; Boydston, A. J., *J Am Chem Soc* **2014,** *136* (4), 1276-1279.
9. Lin, Y.; Kouznetsova, T. B.; Craig, S. L., *J Am Chem Soc* **2019**, 142, (1) 99-103.
10. Kumpfer, J. R.; Taylor, S. D.; Connick, W. B.; Rowan, S. J., *Journal of Materials Chemistry* **2012,** *22* (28), 14196-14204.
11. Beiermann, B. A.; Kramer, S. L. B.; Moore, J. S.; White, S. R.; Sottos, N. R., *ACS Macro Lett* **2012,** *1* (1), 163-166.
12. Nallicheri, R. A.; Rubner, M. F., *Macromolecules* **1991,** *24* (2), 517-525.
13. Choi, S. J.; Kuwabara, J.; Nishimura, Y.; Arai, T.; Kanbara, T., *Chem. Lett.* **2012,** *41* (1), 65-67.
14. Sun, H.; Liu, S.; Lin, W.; Zhang, K. Y.; Lv, W.; Huang, X.; Huo, F.; Yang, H.; Jenkins, G.; Zhao, Q.; Huang, W., *Nature Communications* **2014,** *5*, 3601.
15. Zeng, S.; Sun, H.; Park, C.; Zhang, M.; Zhu, M.; Yan, M.; Chov, N.; Li, E.; Smith, A. T.; Xu, G., *Materials Horizons* **2020**, 7(1), 164-172.
16. Zhang, H.; Zeng, D.; Pan, Y.; Chen, Y.; Ruan, Y.; Xu, Y.; Boulatov, R.; Creton, C.; Weng, W., *Chemical Science* **2019,** *10* (36), 8367-8373.
17. Shree, S.; Dowds, M.; Kuntze, A.; Mishra, Y. K.; Staubitz, A.; Adelung, R., *Materials Horizons* **2020**.
18. Zhang, X.; Wang, J.-Y.; Ni, J.; Zhang, L.-Y.; Chen, Z.-N., *Inorganic Chemistry* **2012,** *51* (10), 5569-5579.
19. Dong, Y.; Zhang, J.; Li, A.; Gong, J.; He, B.; Xu, S.; Yin, J.; Liu, S. H.; Tang, B. Z., *Journal of Materials Chemistry C* **2020**, 8(3), 894-899.
20. Achira, H.; Hoga, Y.; Yoshikawa, I.; Mutai, T.; Matsumura, K.; Houjou, H., *Polyhedron* **2016,** *113*, 123-131.
21. Chatterjee, S.; Norton, A. E.; Edwards, M. K.; Peterson, J. M; Taylor, S. D.; Bryan, S. A; Andersen, A.; Govind, N.; Schmitt, T. E.; Connick, W. B.; Levitskaia, T. G., *Inorg. Chem.* **2015,** *54* (20), 9914-9923.
22. Taylor, S. D.; Norton, A. E.; Hart, R. T.; Abdolmaleki, M. K.; Krause, J. A.; Connick, W. B., *Chemical Communications* **2013,** *49* (80), 9161-9163.
23. Ji, Z. Q.; Li, Y. J.; Pritchett, T. M.; Makarov, N. S.; Haley, J. E.; Li, Z. J.; Drobizhev, M.; Rebane, A.; Sun, W. F., *Chem-Eur J* **2011,** *17* (8), 2479-2491.
24. Yam, V. W. W.; Chan, K. H. Y.; Wong, K. M. C.; Zhu, N. Y., *Chem-Eur J* **2005,** *11* (15), 4535-4543.
25. Du, P., *Inorg. Chim. Acta* **2010,** *363* (7), 1355-1358.
26. Kato, M.; Omura, A.; Toshikawa, A.; Kishi, S.; Sugimoto, Y., *Angewandte Chemie, International Edition* **2002,** *41* (17), 3183-3185.
27. Ni, J.; Wang, Y.G.; Wang, J.Y.; Zhao, Y.Q.; Pan, Y.Z.; Wang, H.H.; Zhang, X.; Zhang, J.J.; Chen, Z.-N., *Dalton Trans.* **2013,** *42* (36), 13092-13100.
28. Jobbagy, C.; Deak, A., *Eur. J. Inorg. Chem.* **2014,** *2014* (27), 4434-4449.
29. Minati, L.; Chiappini, A.; Armellini, C.; Carpentiero, A.; Maniglio, D.; Vaccari, A.; Zur, L.; Lukowiak, A.; Ferrari, M.; Speranza, G., *Materials Chemistry and Physics* **2017,** *192*, 94-99.
30. Abe, T.; Itakura, T.; Ikeda, N.; Shinozaki, K., *Dalton Trans.* **2009,** (4), 711-715.
31. Ni, J.; Zhang, X.; Qiu, N.; Wu, Y.-H.; Zhang, L.-Y.; Zhang, J.; Chen, Z.-N., *Inorg. Chem.* **2011,** *50* (18), 9090-9096.
32. Abdolmaleki, M. K.; Riasi, M. S.; Enayati, M.; Norton, A. E.; Chatterjee, S.; Yeghiazarian, L.; Connick, W. B.; Abbaspourrad, A., *Talanta* **2020,** *209*, 120520.
33. Nguyen, N. D.; Zhang, G.; Lu, J.; Sherman, A. E.; Fraser, C. L., *Journal of Materials Chemistry* **2011,** *21* (23), 8409-8415.
34. Huang, G.; Xia, Q.; Huang, W.; Tian, J.; He, Z.; Li, B. S.; Tang, B. Z., *Angewandte Chemie International Edition* **2019,** *58* (49), 17814-17819.
35. Bailey, J. A.; Miskowski, V. M.; Gray, H. B., *Inorganic Chemistry* **1993,** *32* (4), 369-370.
36. Mathew, I.; Sun, W., *Dalton Transactions* **2010,** *39* (25), 5885-5898.
37. Yip, H.-K.; Cheng, L.-K.; Cheung, K.-K.; Che, C.-M., *Journal of the Chemical Society, Dalton Transactions* **1993,** (19), 2933-2938.

TOC